Science of the Total Environment 918 (2024) 170641

Contents lists available at ScienceDirect

Science of the Total Environment

journal homepage: www.elsevier.com/locate/scitotenv

Towards an integrated view on microbial CH_4, N_2O and N_2 cycles in brackish coastal marsh soils: A comparative analysis of two sites

Mikk Espenberg [a,b,*], Kristin Pille [a], Bin Yang [c], Martin Maddison [a], Mohamed Abdalla [b], Pete Smith [b], Xiuzhen Li [c], Ping-Lung Chan [d], Ülo Mander [a]

[a] Institute of Ecology and Earth Sciences, University of Tartu, Tartu, Estonia
[b] Institute of Biological and Environmental Sciences, University of Aberdeen, Aberdeen, United Kingdom
[c] State Key Laboratory of Estuarine and Coastal Research, Institute of Eco-Chongming, East China Normal University, Shanghai, China
[d] School of Science and Technology, Hong Kong Metropolitan University, Hong Kong, China

HIGHLIGHTS

- Plants affect microbes to emit CH_4, N_2O and N_2.
- n-DAMO mitigated CH_4 emission for *Phragmites*, and *Spartina* and *Scirpus* sites
- N_2O was emitted due to nitrification or incomplete denitrification
- Climate forcing came from CH_4 in vegetated sites and from N_2O in *Phragmites* site
- Nutrient cycles and soil-plant-atmosphere continuum should be studied synchronously

GRAPHICAL ABSTRACT

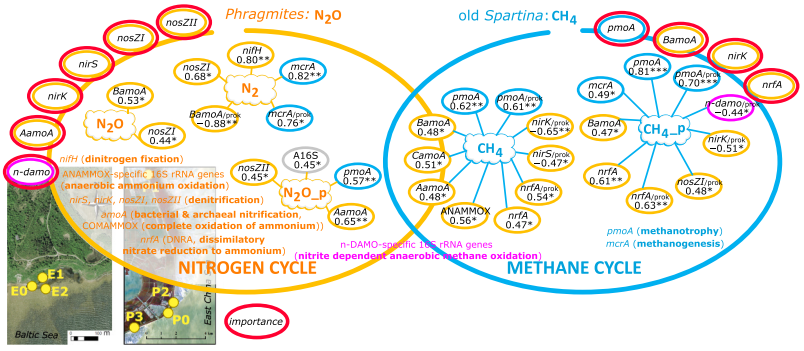

ARTICLE INFO

Editor: Jay Gan

Keywords:
Carbon cycle
Nitrogen cycle
Coastal ecosystems
Nitrous oxide
Methane
Greenhouse gases

ABSTRACT

Coastal ecosystems, facing threats from global change and human activities like excessive nutrients, undergo alterations impacting their function and appearance. This study explores the intertwined microbial cycles of carbon (C) and nitrogen (N), encompassing methane (CH_4), nitrous oxide (N_2O), and nitrogen gas (N_2) fluxes, to determine nutrient transformation processes between the soil-plant-atmosphere continuum in the coastal ecosystems with brackish water. Water salinity negatively impacted denitrification, bacterial nitrification, N fixation, and n-DAMO processes, but did not significantly affect archaeal nitrification, COMAMMOX, DNRA, and ANAMMOX processes in the N cycle. Plant species age and biomass influenced CH_4 and N_2O emissions. The highest CH_4 emissions were from old *Spartina* and mixed *Spartina* and *Scirpus* sites, while *Phragmites* sites emitted the most N_2O. Nitrification and incomplete denitrification mainly governed N_2O emissions depending on the environmental conditions and plants. The higher genetic potential of ANAMMOX reduced excessive N by converting it to N_2 in the sites with higher average temperatures. The presence of plants led to a decrease in the N fixers' abundance. Plant biomass negatively affected methanogenetic *mcrA* genes. Microbes involved in n-DAMO processes helped mitigate CH_4 emissions. Over 93 % of the total climate forcing came from CH_4 emissions, except for the Chinese bare site where the climate forcing was negative, and for *Phragmites* sites, where almost 60 % of

* Corresponding author at: Institute of Ecology and Earth Sciences, University of Tartu, Tartu, Estonia.
E-mail addresses: mikk.espenberg@ut.ee, mikk.espenberg@abdn.ac.uk (M. Espenberg).

https://doi.org/10.1016/j.scitotenv.2024.170641
Received 17 September 2023; Received in revised form 29 January 2024; Accepted 31 January 2024
Available online 6 February 2024

the climate forcing came from N_2O emissions. Our findings indicate that nutrient cycles, CH_4, and N_2O fluxes in soils are context-dependent and influenced by environmental factors and vegetation. This underscores the need for empirical analysis of both C and N cycles at various levels (soil-plant-atmosphere) to understand how habitats or plants affect nutrient cycles and greenhouse gas emissions.

1. Introduction

Coastal environments provide unique natural habitats, services and resources for many organisms and favourable conditions for human settlement (Winter et al., 2019), with about 40 % of the global population living within 100 km of the coast (Bruns, 2014). Coastal habitats face local and global risks from both direct (e.g., temperature, rainfall, water quality disturbances) and indirect (e.g., sea-level rise, coastal erosion) factors linked to environmental and climate changes (Burden et al., 2020; Zhu et al., 2020; Liu et al., 2021), and rapid urbanisation have amplified these impacts (Craig-Smith et al., 2006). Human coastal habitats often lie within river deltas (e.g., Shanghai) or have limited oceanic connections despite receiving substantial riverine inputs (e.g., Baltic Sea), resulting in lower water salinity and slower pollutants dispersion compared to the open oceans, making it important to study those urbanised coasts with brackish water (mixed saline and freshwater) greatly impacted by pollution (Yang et al., 2020; Jaspers et al., 2021). Excessive nutrient pollution from agricultural, industrial, and domestic sources is a major concern for coastal ecosystems, impacting their ecological integrity and biodiversity globally (Deegan et al., 2012; Newton et al., 2020). These pollutants primarily enter coastal zones through riverine contamination, atmospheric deposition, and direct dumping (Paerl et al., 2002; Lapointe et al., 2015; Guibert et al., 2016). This poses a significant threat as it can fundamentally change the functioning and appearance of coastal ecosystems (Herbert, 1999; Bauer et al., 2013).

In coastal ecosystems, losing diversity and foundational plant species can severely undermine their resilience to climate change and other pressures (Bernhardt and Leslie, 2013). Plant-microbe interactions, crucial for the diversity of coastal ecosystems by shaping both plant rhizobiomes and microbial communities, remain largely unexplored (Sasse et al., 2018). The microbial community in coastal areas is sensitive to environmental shifts and plays a role in regulating the success of invasive plant species (Kowalski et al., 2015; Gribben et al., 2017; Novoa et al., 2020). Conversely, coastal vegetation influences microbial processes, especially in controlling emissions of nitrous oxide (N_2O) and methane (CH_4) (Al-Haj and Fulweiler, 2020; Hsieh et al., 2021). These gases can efficiently move through the leaves, stems, and rhizomes of plants with aerenchyma to the atmosphere, a characteristic common in many wetland plants (Cheng et al., 2007).

N_2O and CH_4, potent greenhouse gases, show varying emissions from coastal areas depending on microbial communities and their influencing factors (Cavicchioli et al., 2019; Quick et al., 2019; Wallenius et al., 2021). It has been shown that the same invasive species, e.g. *Spartina alterniflora*, may have climate cooling or warming effects on climate due to changes in N_2O (Yang et al., 2020) and CH_4 emissions (Yang et al., 2021), emphasising the need for a comprehensive view of any species' impact on the atmosphere. Global coastal wetlands CH_4 emissions were estimated at 5.3–6.2 Tg CH_4 y^{-1} (Al-Haj and Fulweiler, 2020), constituting around 60 % of the global marine CH_4 budget and < 7 % of the global wetland CH_4 budget (Saunois et al., 2020). In contrast, estuarine environments, including coastal wetlands, are a relatively minor source of global N_2O, 0.31 Tg N_2O-N y^{-1} or < 2 % of the total anthropogenic source, although it is expected to double in the short-term future (Murray et al., 2015).

Carbon (C) and nitrogen (N) cycling are tightly coupled at the microbial and plant levels in all ecosystems. Still, these two key elemental cycles are very often studied separately (Cavicchioli et al., 2019). Soil microbial C and N dynamics are altered in a changing climate due to soil warming, changes in root exudates and hydrology, and disturbances, including pollution (Jansson and Hofmockel, 2020). It is crucial to advance our understanding of C and N cycling interactions in coastal environments to better protect and manage the coastal areas.

Widely acknowledged processes in C (methanogenesis, methanotrophy) and N cycles (denitrification, nitrification, N fixation), along with recently more investigated processes such as dissimilatory nitrate reduction to ammonium (DNRA) and anaerobic ammonium oxidation (ANAMMOX) (both part of N cycle), have gained significant attention in coastal studies (Damashek and Francis, 2018; Wallenius et al., 2021). New processes like nitrate/nitrite-dependent anaerobic methane oxidation (n-DAMO; directly combines C and N cycles) and complete oxidation of ammonium to nitrate (COMAMMOX; part of N cycle) still need investigation to assess their roles in various ecosystems (in't Zandt et al., 2018), including coastal regions. CH_4 emissions primarily depend on the balance between methanogenesis, methanotrophy, and n-DAMO (Wallenius et al., 2021). However, incomplete denitrification, nitrification, and DNRA are key microbial pathways that may significantly contribute to N_2O production (Bahram et al., 2022). The interactions among all these processes will determine gas fluxes.

The coastal zone, acting as the meeting point between land and ocean, is affected by marine, terrestrial and atmospheric processes (Winter et al., 2019). Due to the diverse aspects requiring consideration in coastal studies – such as water, soil, vegetation, and gas – there is a significant lack of comprehensive studies covering all these elements. Moreover, the integration of microbial C and N cycles across coastal ecosystems presents a significant yet needed challenge. Understanding microbial processes in nutrient cycling with plants is crucial for sustaining the functionality of coastal areas. Here are the two main novelties of this study: 1) A comprehensive microbial analysis study is conducted for Chinese and Estonian coastal sites under varied vegetation, incorporating CH_4 and N_2O fluxes as background data to describe the potential activity of different functional genes. CH_4 and N_2O fluxes are direct products of different processes involving these key genes, with the microbial analysis primarily focused on in this study and highlighting deterministic processes behind them. An integrated view of microbial C and N cycles is another advantage. 2) This study emphasises the importance of studying CH_4 and N_2O cycles together, underlining their significance in contributing to global warming. Another primary focus is contextualising these highly contributing greenhouse gases (CH_4 and N_2O), aiming to discern their differences and collective contribution to global warming.

The general aims of this study are to identify and assess the microbial processes contributing to greenhouse gases and examine how plants relate to functional gene abundances and greenhouse gases in coastal zones with brackish water. It focuses on analysing soil bacteria and archaea abundance, along with their functional genes, to understand nutrient transformation processes across the soil-plant-atmosphere continuum. The hypotheses of this study are as follows: 1) Aquatic macrophytes determine microbiome composition and CH_4 and N_2O fluxes in coastal soils. 2) CH_4 and N_2O cycles in coastal soils affect each other. 3) Understudied microbial processes, such as n-DAMO and COMAMMOX, play an important role in CH_4 and N_2O fluxes within coastal ecosystems.

2. Methods

2.1. Description of the study sites

Seven coastal zones with different plant species or bare soils in Pivarootsi, Estonia (58.535864° N, 23.606722° E) (Fig. 1A) and Shanghai, China (30.833333° N, 121.833333° E) (Fig. 1B) were selected as study sites. All studied sites were similarly affected by the brackish water, with water salinity around 7–8 ‰ (Yang et al., 2020; Jaspers et al., 2021). The Estonian and Chinese sites have an average annual temperature of 6.8 °C and 15.9 °C and an annual precipitation of 761 and 1150 mm, respectively. Each site comprised three sampling points, either in bare sites or dominated by the *Schoenoplectus tabernaemontanii* and *Phragmites australis* in Estonia, or *Spartina alterniflora* and *Scirpus mariqueter* in China. In this study, our primary focus is on the microbiological analyses of samples from Estonian and Chinese sites. While data regarding N_2O (Yang et al., 2020) and CH_4 (Yang et al., 2021) in the Chinese sites have been previously described, we present a more comprehensive description of the data from the Estonian sites.

The coastal sites are named according to dominant plant species as follows: bare (E0), *Phragmites australis* (E1), and *Schoenoplectus tabernaemontanii* (E2) in Estonia; bare (P0), a mix of *Spartina alterniflora* and *Scirpus mariqueter* (P1), old *Spartina alterniflora* (P2), and young *Spartina alterniflora* (P3) in China. Native plant species populate these sites, except for *S. alterniflora*, which has rapidly spread in China. Invasive *S. alterniflora* colonised P1 and P2 nine years prior to the study and invaded P3 three years before. Hereafter, we refer to P2 and P3 as the old and young *Spartina* sites, respectively. Detailed descriptions of these Chinese coastal sites can be found in Yang et al. (2020) and Yang et al. (2021). In Estonia, fieldwork took place during the intensive plant growth period between June and September 2019. The air temperature ranged from 16 to 24 °C, and water level fluctuations of 0–30 cm were observed during the sampling days.

2.2. Sampling and analyses of water, soil, and plants

A detailed description of water parameters (including water salinity, electrical conductivity, NO_3^-, NO_2^-, NH_4^+), soil parameters (such as temperature, salinity, and total nitrogen (TN)) and plant sample collection and analysis is available in Yang et al. (2020).

At each Estonian sampling site, the water table dynamics were measured using perforated polypropene pipes (Ø 75 mm) as monitoring wells. The following parameters were measured using a handheld portable YSI Professional Plus for each sampling: temperature (°C), pH, electrical conductivity (μS/cm), redox potential, and dissolved oxygen content (mg/L) from the well water. Soil temperature was recorded at a depth of 10 cm with a temperature logger (Comet Systems Ltd., Rožnov pod Radhoštem, Czech Republic). All measurements were conducted twice a month throughout the study period in Estonia.

Soil samples from Estonia (0–10 cm depth) were collected at the end of the study (27.09.2019). Samples for chemical analyses were stored at 4 °C, and microbiological samples were stored at −20 °C until further analyses. Soil pH, organic matter (OM), TN, NO_3^-, NH_4^+, total phosphorus (TP), potassium (K), calcium (Ca), and magnesium (Mg) contents were measured with the standard methods (APHA-AWWA-WEF, 2005) in the Plant Biochemistry Laboratory of the Estonian University of Life Sciences. Soil pH was determined using a 1 N KCl solution; NH_4^+ and NO_3^- were determined on a 2 M KCl extract of soil by flow-injection analysis. OM content of dry matter was determined by loss on ignition. TN and TC contents of oven-dry samples were determined by a dry-combustion method on a varioMAX CNS elemental analyser (Elementar Analysensysteme GmbH, Germany). TP (NH_4-lactate extractable) was determined on a FiaStar5000 flow-injection analyser. K was determined from the same solution by the flame-photometric method and Mg was determined from a 100 mL NH_4-acetate solution with a titanium-yellow reagent on the flow-injection analyser. Ca was analysed using the same solution by a flame-photometrical method.

For both Estonian and Chinese soil samples, the concentrations of total carbon (TC), total organic carbon (TOC), dissolved carbon (DC), dissolved organic carbon (DOC) and dissolved nitrogen (DN) were determined using a Vario TOC (Elementar GmbH, Germany).

In the Estonian sites, plant height and density were evaluated bimonthly throughout the study. At the end of the study, above- and belowground biomass stocks were measured in the E1 (*Phragmites*) and E2 (*Schoenoplectus*) sites. The aboveground biomass was harvested on three subplots (0.2 m^2), while the belowground biomass (roots and rhizomes) was determined from nine soil cores (0.01 m^2) taken to a depth of 20 cm using a shovel from both coastal marsh sites. After manually washing each core over a 0.5 mm mesh sieve to remove the bulk soil, roots and rhizomes were manually picked from the residual soil. The collected above- and belowground biomass samples were oven-dried at 70 °C until a constant weight was achieved. Subsequently, the biomass amounts were analysed for N and P concentrations using standard methods (APHA-AWWA-WEF, 2005) at the Plant Biochemistry Laboratory of the Estonian University of Life Sciences.

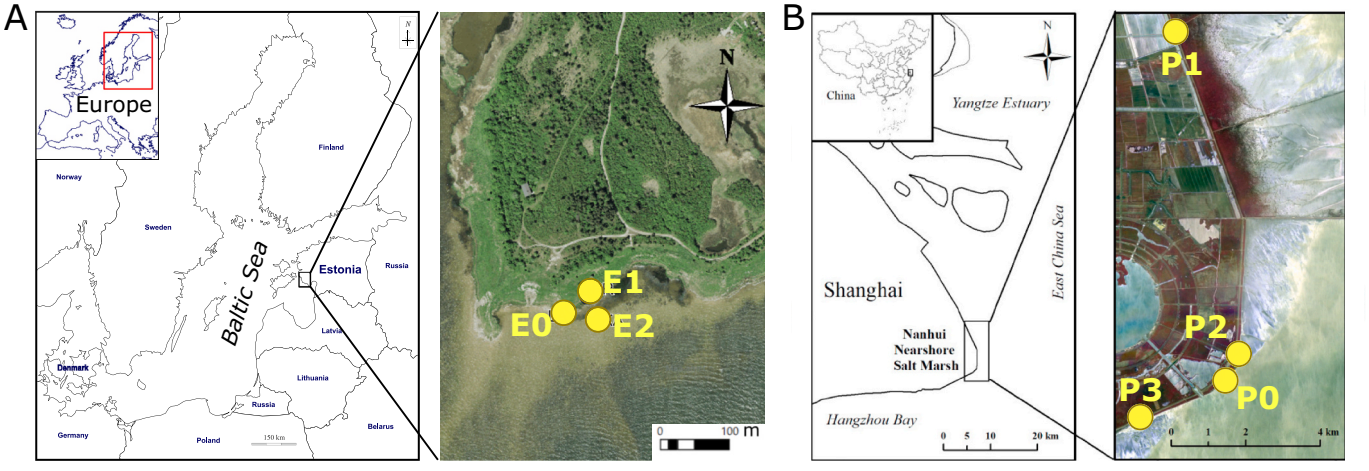

Fig. 1. (A) Location of the three sampling plots in the Pivarootsi coast of the Baltic Sea, Estonia (Photo by Estonian Land Board). Sites: bare (E0), *Phragmites australis* (E1), and *Schoenoplectus tabernaemontanii* (E2). (B) Location of the four sampling plots in the Nanhui coast of the Yangtze estuary, Shanghai, China (Photo by RapidEye Satellite). Sites: bare (P0), a mix of *Spartina alterniflora* and *Scirpus mariqueter* (P1), old *Spartina alterniflora* (P2), and young *Spartina alterniflora* (P3).

2.3. Soil DNA extraction

DNA was extracted from the Estonian and Chinese soil samples using the PowerSoil DNA Isolation kit (MO BIO Laboratories Inc., Carlsbad, CA, USA), following the manufacturer's protocol. The homogenisation step was performed at 5000 rpm for 20 s using Precellys® 24 (Bertin Technologies, France). Extracted DNA from samples was stored at −20 °C until further analyses. The quality and quantity of the extracted DNA were assessed using a spectrophotometer Infinite M200 (Tecan AG, Austria). DNA concentrations were determined by measuring the difference in light flux intensity directed at and through the samples. The sample's purity was evaluated by the ratio of the absorbance values measured at 260 nm to 280 nm.

2.4. Quantitative PCR

Real-time quantitative polymerase chain reaction (qPCR) was used to amplify the 16S rRNA gene, assessing bacterial and archaeal community abundance (Supplementary Table 1). For estimation of denitrification (*nirK*, *nirS*, *nosZI*, *nosZII*), nitrification (bacterial *amoA*, archaeal *amoA*, COMAMMOX *amoA*), DNRA (*nrfA*), anaerobic ammonium oxidation (ANAMMOX-specific 16S rRNA) and N fixation (*nifH*), the respective functional genes were quantified using qPCR. n-DAMO process was determined via n-DAMO specific 16S rRNA genes by applying the qPCR. Methanogenic *mcrA* and methanotrophic *pmoA* genes were quantified with the qPCR.

qPCR assays were performed using RotorGene® Q equipment (Qiagen, USA). Amplifications were carried out in 10 μL reaction solutions containing 5 μL Maxima SYBR Green Master Mix (Thermo Fisher Scientific Inc., USA), with optimised forward and reverse primer concentrations, 1 μL template DNA and sterile distilled water. The gene-specific primer sets, optimised primer concentrations, and thermal cycling conditions for each target gene are shown in Supplementary Table 1. All qPCR measurements were performed in triplicate, and the absence of contaminations was verified against negative controls. Standard curves for each target gene were prepared from serially diluted stock solutions of target sequences (Eurofins MWG Operon, Germany).

Quantitative data were analysed with RotorGene Series Software v. 2.0.2 (Qiagen) and the LinRegPCR program v. 2020.01 (Ruijter et al., 2009). Gene abundances were calculated as the mean fold differences between samples and corresponding 10-fold standard dilution in respective standards, as recommended by Ruijter et al., 2009; gene abundances were reported as gene copy numbers per gram of dry soil (copies/g dw). The abundance of total prokaryotes was calculated by summing the bacterial and archaeal 16S rRNA gene abundances. Additionally, the proportions of organisms with certain functional traits in the prokaryotic communities were estimated by normalising the functional gene abundances with the 16S rRNA genes of the bacteria and archaea.

2.5. Sampling and analyses of gas

Gas samples were collected from Estonian and Chinese sites to determine N_2O and CH_4 emissions. The emission measurements for Chinese coastal areas are thoroughly described in Yang et al. (2020) and Yang et al. (2021), respectively.

For the Estonian sites,

N_2O and CH_4 emissions at the Estonian sites were measured in situ twice a month during the study period using static closed chambers (Ø 50 cm, height 70 cm and volume 82 L for bare (E0) and *Schoenoplectus* (E2) sites, and an additional chamber elevation was used with height 50 cm and volume 99 L for *Phragmites* (E1) site) sealed with a water-filled collar on the soil surface. Gas samples were taken immediately after closing the chambers and after 20, 40 and 60 min using pre-evacuated (0.3 mbar) 50-mL gas bottles. Gas concentration analysis was determined using the Shimadzu GC-2014 gas-chromatographic system (electron capture detector (ECD), flame ionisation detector (FID)) combined with a Loftfield autosampler (Loftfield et al., 1997).

During the soil sampling session, an intact soil core from the 0–10 cm soil layer of each sampling plot was collected into a stainless-steel cylinder (Ø 6.8 cm) to measure potential N_2 fluxes with helium atmosphere soil incubation technique (Swerts et al., 1995; Butterbach-Bahl et al., 2002). The cylinders with the intact soil cores were placed into special gas-tight incubation vessels located in the temperature-controlled chamber in the laboratory. Gases were removed by flushing with an artificial gas mixture (21.0 % O_2, 358 ppm CO_2, 0.313 ppm N_2O, 1.67 ppm CH_4, 5.97 ppm N_2 and rest He). The new atmosphere equilibrium was established by continuously flushing the vessel headspace with the artificial gas mixture at 20 mL per min after 12–24 h, and the flushing time depended on the soil moisture. The incubation temperature simulated field conditions. A gas-chromatograph (Shimadzu GC-2014) equipped with a thermal conductivity detector was used to measure N_2 concentration in the mixture of emitted gases accumulated in the headspace (start value, 40 min, 80 min and 120 min as final value) of the cylinder after 2 h of closure. Intact soil core flux rate calculation was based on the formula used in Butterbach-Bahl et al. (2002).

The total emissions of CH_4 and N_2O were calculated in kg CO_2eq ha^{-1} y^{-1} using the global warming potential over a 100-year time horizon (GWP_{100}) of 27.2 and 273, respectively (IPCC, 2021).

2.6. Data analyses

R version 4.1.0 (R Core Team, 2021) was used for data analysis and visualization. Statistical significance was determined at $p < 0.05$. Principal component analysis (PCA) was performed on gene parameters using ade4 v. 1.7–17 (Dray and Dufour, 2007) to reduce the number of variables of a data set, while preserving as much information as possible. PCA was based on the target gene abundances (bacterial and archaeal 16S rRNA, *nirK*, *nirS*, *nosZI*, *nosZII*, bacterial *amoA*, archaeal *amoA*, COMAMMOX *amoA*, *nrfA*, ANAMMOX-specific 16S rRNA, *nifH*, n-DAMO specific 16S rRNA, *mcrA*, and *pmoA* genes) and the target gene proportions in the prokaryotic community, and gas emissions used as passive variables. Differences in PCA between the sites were evaluated using PERMANOVA with 9999 permutations (vegan v. 2.5–7) (Oksanen et al., 2020). Linear mixed-effects models were applied using "lmer" v. 1.1–31 (Bates et al., 2015) to investigate differences in gas flux measurements between the sites, incorporating both temporal (sampling days) and spatial (sampling points) effects as random factors. *P*-values were calculated using the lmerTest v. 3.1-3 (Kuznetsova et al., 2017) to confirm the significance of the relationships. Spearman's rank correlation coefficient was used to compare gene parameters, environmental variables, and GHG fluxes. P-values were considered statistically significant after Benjamin–Hochberg correction. A one-way analysis of variance with Tukey HSD post hoc tests was used to evaluate the significance of the differences between sites in gene parameters, physicochemical parameters and emission values, and logarithmic transformation was applied if necessary. Random forest analysis with 100 replications was conducted using Boruta v. 7.0.0 (Kursa and Rudnicki, 2010) to identify the gene parameters that best predicted CH_4 and N_2O fluxes.

3. Results

3.1. Soil and plants physicochemical characteristics, and gas (CH_4, N_2O and N_2) fluxes

The physicochemical parameters of soil and plants in Estonia and China are detailed in Supplementary Tables 2, 3 and 4, with the Chinese sites described by Yang et al. (2020). In Estonia, the water level fluctuations during the measurement period ranged from −29 to 30 cm. At the bare (E0) site, water levels varied from −22 to 4 cm, in the *Phragmites* (E1) site from −28 to 5 cm, and in the *Schoenoplectus* (E2) site from

0 to 30 cm, with the most significant changes observed in July. The water temperature measured across all areas ranged from 9.3 to 17.8 °C. Water pH levels averaged between 6.4 and 7.2, with the highest values found in the *Schoenoplectus* (E2) site. Dissolved oxygen content in the water was 2.0 ± 0.8 mg/L in the bare (E0) site, 1.3 ± 0.4 mg/L in the *Phragmites* (E1) site and 5.7 ± 5.1 mg/L in the *Schoenoplectus* (E2) site throughout the measurement period. Electrical conductivity varied between 11,587.3 ± 2362.5 uS/cm in the bare (E0) site, 9744.0 ± 1162.6 uS/cm in the *Phragmites* (E1) site, and 9587.3 ± 1633.99 uS/cm in the *Schoenoplectus* (E2) site. The redox potential in water was −179.9 ± 62.6 in the bare (E0) site, −237.0 ± 41.0 mV in the *Phragmites* (E1) site and − 65.0 ± 132.0 mV in the *Schoenoplectus* (E2) site throughout the measurement period.

In Estonian sites, the soil temperature ranged from 8.8 to 26.6 °C. The average soil temperatures were 18.5 ± 5.1 °C in the bare (E0) site, 16.2 ± 3.5 °C in the *Phragmites* (E1) site and 19.2 ± 5 0.5 °C in the *Schoenoplectus* (E2) site. Comparatively, soil temperatures measured in China were slightly higher, averaging 18.9 ± 8.6 °C in the bare (P0) site, 20.4 ± 8.8 °C in the *Spartina* and *Scirpus* (P1) site, 19.8 ± 8.9 °C in the old *Spartina* (P2) site and 21.3 ± 8.2 °C in the young *Spartina* (P3) site. In Estonian sites, the TC values in the soil were almost four times higher than those in the Chinese areas (Supplementary Table 2). The greatest statistical differences among the sites were in TC and TOC values compared to others (DOC, DC, and DN) (Supplementary Table 3).

On sampling days, *Phragmites* (E1) showed an average plant height of 135.8 ± 7.0 cm, while *Schoenoplectus* (E2) averaged 67.7 ± 10.1 cm. *Phragmites* (E1) had a plant density of 177.6 ± 8.1 plants per 0.2 m^2, whereas *Schoenoplectus* (E2) had 122.3 ± 90.9 plants per 0.2 m^2. Soil pH ranged from 6.8 to 7.4 in the Estonian sites, with lower values measured in the *Phragmites* (E1) site (Supplementary Table 4). Concentrations of NH_4^+, P, K, Ca and Mg in soils ranged from 2.1 to 10.5 mg/kg, 20.9 to 67.0 mg/kg, 150.4 to 41.1 mg/kg, 1785.9 to 2023.7 mg/kg and 242.3 to 846.3 mg/kg, respectively. All sites differed statistically significantly in K and Ca concentrations. The content of OM in the soils ranged from 2.6 to 10.4 %, with the highest values recorded in the *Phragmites* (E1) site. TN content ranged from 0.2 to 0.5 % in soil samples, showing significant differences among sites. On average, the belowground and aboveground biomass ratios under dry conditions were 0.14 and 0.05 for *Phragmites* (E1) and *Schoenoplectus* (E2) sites, respectively. In *Phragmites* (E1), roots and plants showed higher TP and TN contents than *Schoenoplectus* (E2).

The Chinese bare (P0) sites showed distinct differences, primarily exhibiting higher NO_3^- and water salinity as detailed in Yang et al. (2020). The *Spartina* and *Scirpus* (P1) site had higher sediment salinity, sediment moisture, TOC and NH_4^+ values compared to other plots. The old *Spartina* (P2) and young *Spartina* (P3) sites displayed higher sediment temperature values and lower TC concentrations than the other plots.

In Estonia, CH_4 emissions varied between 3.1 and 1538.7 μgC m^{-2} h^{-1} (Fig. 2A), peaking in July and reaching their lowest levels in June and August. The bare (E0) site showed the highest CH_4 emissions. There was a significant difference in CH_4 emissions between the *Phragmites* (E1) site and both the bare (E0) ($p < 0.001$) and *Schoenoplectus* (E2) sites ($p < 0.01$), with lower emissions recorded at the *Phragmites* (E1) site. Chinese coastal sites displayed much higher CH_4 emissions, ranging from −1741 to 72,170 μgC m^{-2} h^{-1}, predominantly from the old *Spartina* (P2) site (Fig. 2B). All sites showed significant differences in CH_4 emissions from each other (all $p < 0.001$, except P1 and P3 ($p < 0.05$)). Detailed CH_4 emission data from the Chinese sites can be found in Yang et al. (2021). The total emissions, in kg CO_2eq ha^{-1} y^{-1}, of CH_4 were 521, 92 and 201 for bare (E0), *Phragmites* (E1) and *Schoenoplectus* (E2) sites, and − 1918, 11,737, 70,217 and 2532 for bare (P0), a mix of *Spartina* and *Scirpus* (P1), old *Spartina* (P2) and young *Spartina* (P3) sites, respectively.

In the Estonian sites, the *Phragmites* (E1) site demonstrated

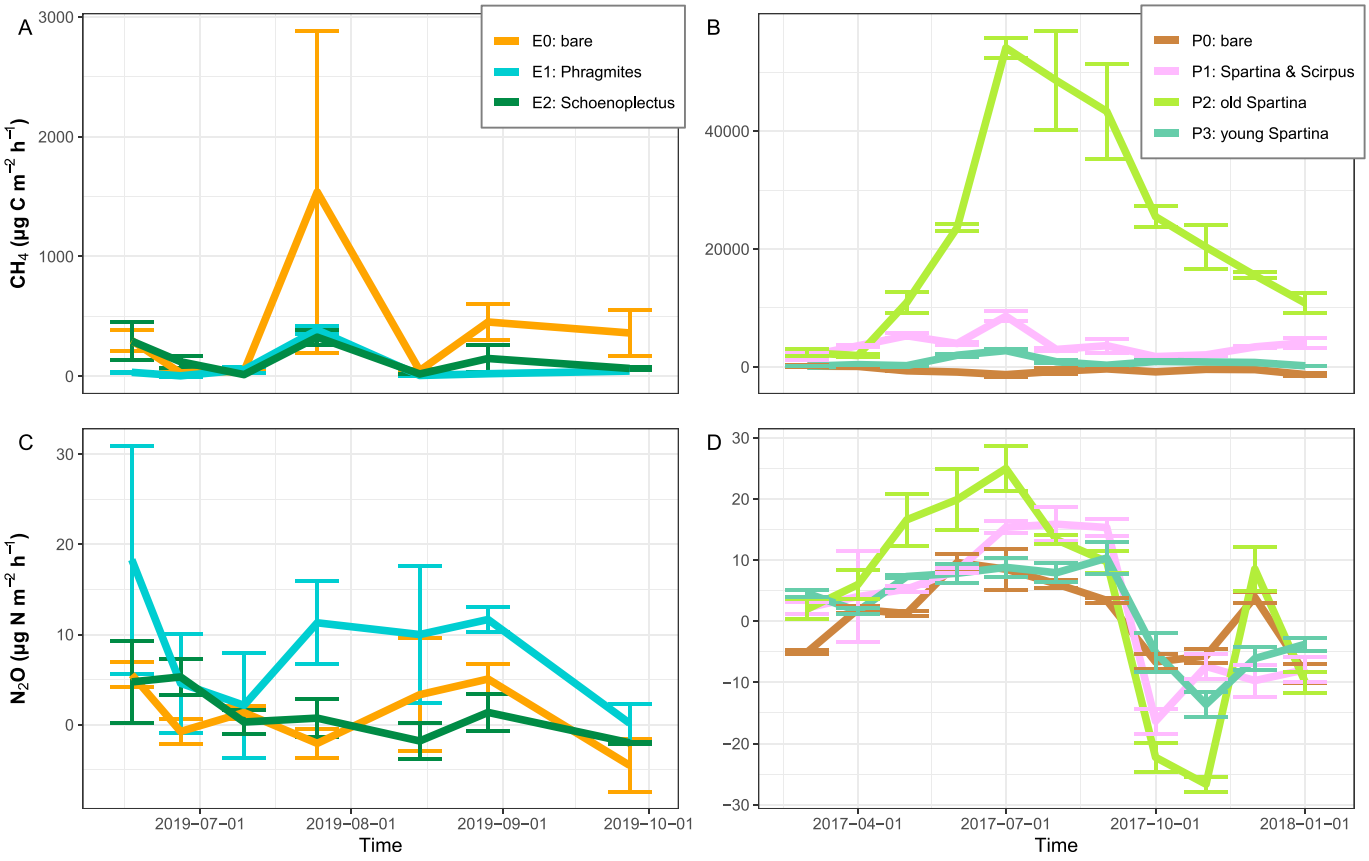

Fig. 2. Dynamics of methane (CH_4) (A, B) and nitrous oxide (N_2O) (C, D) flux in the studied Estonian (A, C) and Chinese (B, D) coastal sites.

significantly higher N_2O emissions compared to the bare ($p < 0.01$) and *Schoenoplectus* (E2) sites ($p = 0.05$) (Fig. 2C). The highest N_2O emission values were measured in June across all sites. In the Chinese coastal sites, the old *Spartina* (P2) site emitted significantly more N_2O compared to the bare ($p < 0.05$) and young *Spartina* (P3) sites ($p < 0.01$) (Fig. 2D). During the warmer summer months (June to September), N_2O emissions peaked, while the lowest levels were observed in October and November. Additional data on N_2O emissions from Chinese sites can be found in Yang et al. (2020). The total emissions, in kg CO_2eq ha^{-1} y^{-1}, of N_2O were 0.7, 125.8 and 13.5 for bare (E0), *Phragmites* (E1) and *Schoenoplectus* (E2) sites, and 8.0, 69.5, 122.4 and 64.1 for bare (P0), a mix of *Spartina* and *Scirpus* (P1), old *Spartina* (P2) and young *Spartina* (P3) sites, respectively.

N_2 emissions from the Estonian bare (E0) sites, *Phragmites* (E1) site and *Schoenoplectus* (E2) site were 2253.3 ± 754.4 μgN m^{-2} h^{-1}, 850.7 ± 105.0 μgN m^{-2} h^{-1} and 614.0 ± 137.3 μgN m^{-2} h^{-1}, respectively.

3.2. Abundance and proportion of soil prokaryotes

The groupings of the different sites based on the gene parameters are depicted in Fig. 3. Bacterial and archaeal abundances were higher in the *Phragmites* (E1) and *Spartina* and *Scirpus* (P1) sites, and lower in the bare (P0) site of the Chinese coast (Fig. 3A, Supplementary Table 5 and 6). In addition, low numbers of archaea were found in the *Schoenoplectus* (E2) site.

The highest abundances of *mcrA* gene copies were found in the Estonian bare (E0) site and the Chinese *Spartina* and *Scripus* (P1) site, with *mcrA* gene copies remaining below the detection limit in the *Phragmites* (E1) and *Schoenoplectus* (E2) sites (Fig. 3A, Supplementary Table 5 and 6). However, *pmoA* genes were detected in all sites, with the highest abundances in the vegetated sites along the Chinese coasts. The n-DAMO-specific 16S rRNA gene copy numbers were higher in the *Phragmites* (E1) and *Spartina* and *Scripus* (P1) sites compared to other sites. Regarding the prokaryotic community, the proportion of the *mcrA* gene was the highest in the bare (E0, P0) sites, while the *pmoA* gene proportion was the highest in the old and young *Spartina* (P2, P3) sites (Fig. 3B, Supplementary Table 5 and 6). The n-DAMO-specific 16S rRNA gene proportion in the prokaryotic community was similar in all the sites.

Denitrification-related genes (*nirK*, *nirS*, *nosZI*, *nosZII*) were generally more abundant in the Estonian than in Chinese sites. However, the abundances of the nitrification genes (different *amoA* genes) were higher in the Chinese sites (Fig. 3A, Supplementary Table 5 and 6). The *nrfA* gene abundance was lowest in the Estonian sites and the bare (P0) site in China. In the Chinese bare (P0) and old *Spartina* (P2) sites, *nifH* abundances were the lowest compared to other sites. The ANAMMOX-specific 16S rRNA genes were present only in Chinese sites. In the prokaryotic community, Estonian sites had higher *nir* genes proportions, but lower *nosZ* genes proportions than Chinese sites (Fig. 3B, Supplementary Table 6 and 7). Bacterial and COMAMMOX *amoA* gene proportions were higher along Chinese coasts, while the archaeal *amoA* gene proportions were consistent across all sites. In the prokaryotic community, the proportion of ANAMMOX-specific 16S rRNA genes was the highest in the Chinese bare (P0) site. The *nrfA* gene proportions were the highest in vegetated Chinese coastal sites, while proportions of *nifH* and n-DAMO-specific 16S rRNA genes were similar across all sites.

3.3. Relationships between gene parameters and environmental characteristics

3.3.1. Relationships between gene, soil, water and plant parameters

The abundances of bacterial and archaeal 16S rRNA genes were positively linked (Supplementary Table 8). The parameters of denitrification genes, including *nirK*, *nirS*, *nosZI*, and *nosZII*, were positively correlated. Bacterial and COMAMMOX *amoA* gene copies displayed a positive relationship. Additionally, the abundances of *nifH* and all denitrifying genes were positively associated. ANAMMOX-specific 16S rRNA gene copies showed a positive relationship with bacterial and COMAMMOX amoA gene copies, but this relationship was negative in the case of archaeal *amoA* gene copies. The increase in *nirK* genes had a negative impact on COMAMMOX *amoA* gene copies. Moreover, n-DAMO-specific 16S rRNA gene abundances were positively associated

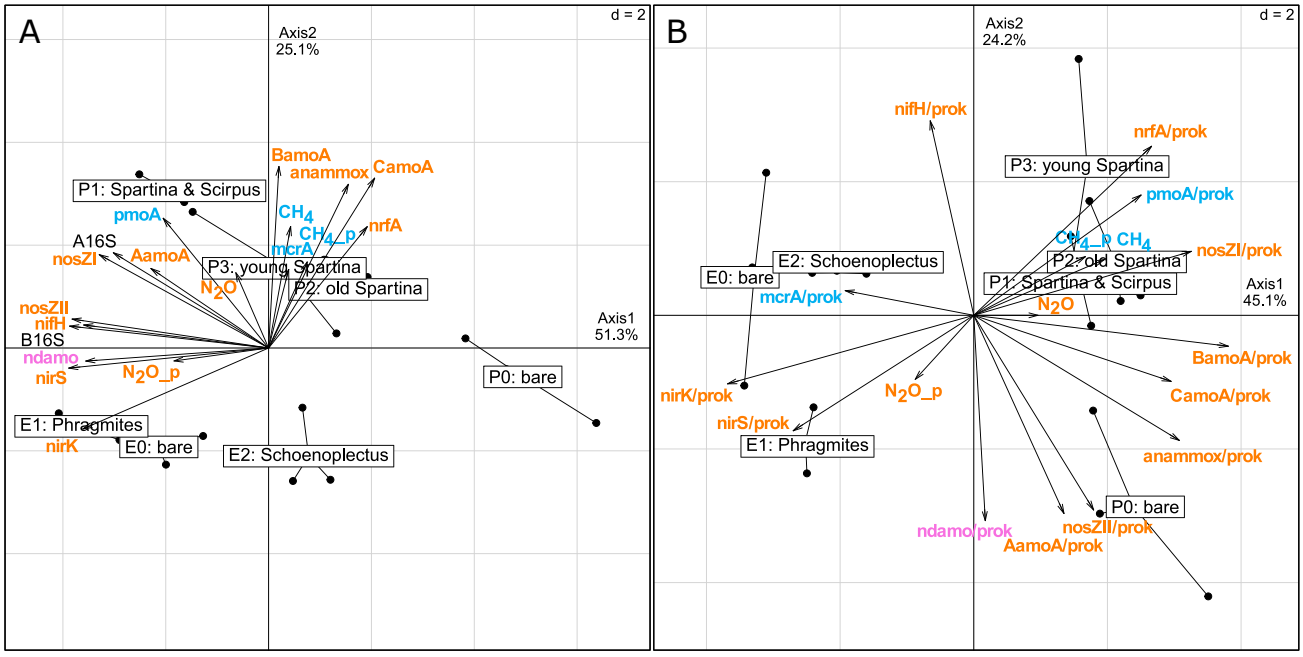

Fig. 3. Clustering of the coastal sites based on principal components analysis (PCA) of the target gene abundances (A) and the target gene proportions in the prokaryotic community (B). Blue color stands for methane cycle processes, orange for nitrogen cycle processes and pink for processes of both cycles. Codes of the coastal sites can be found in the Methods. Gas emissions used as passive variables. Abbreviations: B16S – bacterial 16S rRNA gene, A16S – archaeal 16S rRNA gene, BamoA – bacterial *amoA*, AamoA – archaeal *amoA*, CamoA – COMAMMOX *amoA*, CH_4 or N_2O – same day emission, CH_4_p or N_2O_p – average emission through the study period, d – grid scale.

with archaeal *amoA*, *nifH* and denitrifying genes. *pmoA* genes exhibited a positive association with *nrfA* genes. The *mcrA* gene did not show any correlations with other genes.

Statistically significant relationships between different gene parameters and physicochemical and plant characteristics are shown in Supplementary Tables 9 and 10. The abundances of all genes were highly affected by soil chemical parameters, as several significant relationships were identified. Water salinity decreased gene copy numbers. Plant biomass and nutrients increased the abundance of bacterial *amoA* genes but decreased gene parameters of *mcrA* and *nifH*.

3.3.2. Relationships between gene parameters and gas fluxes

Statistically significant correlations between gene parameters and gas fluxes are shown in Fig. 4. All marker genes involved in the CH_4 cycle - *mcrA*, *pmoA* and n-DAMO-specific 16S rRNA - correlated with the CH_4 fluxes. Of these, microbes possessing *mcrA* genes and *pmoA*-type methanotrophs showed positive associations with CH_4 fluxes, while the n-DAMO process indicated a negative relationship. Moreover, various genes related to N cycle processes (nitrification, denitrification, ANAMMOX, COMAMMOX, and DNRA) were statistically significantly positively or negatively associated with different CH_4 values.

N_2O fluxes were significantly affected by bacterial and archaeal *amoA* genes as well as *nosZ* gene copies (Fig. 4). In addition, a statistically significant association was found between *pmoA* gene copies and the mean N_2O flux of the study period. N_2 emissions showed positive relationships with *nosZI* and *nifH* gene copies but a negative correlation with bacterial *amoA* gene copies (Fig. 4). *mcrA* gene parameters also showed positive correlations with N_2 emission.

The importance of gene parameters in estimating CH_4 and N_2O was investigated, and the ranking of each parameter shows how important it is for predicting the respective greenhouse gas (Fig. 5). The most important parameters found were sites (i.e., different plant cover), *nirK*, bacterial *amoA*, *nrfA* and *pmoA* for CH_4, and archaeal *amoA*, *nirK*, *nirS*, *nosZI*, *nosZII*, n-DAMO-specific 16S rRNA and sites for N_2O.

4. Discussion

4.1. Microbial methane and nitrogen cycle processes of coastal soils

Many relationships between TC, DOC, N, and various microbial processes, including denitrification, nitrification, N fixation, DNRA, ANAMMOX, n-DAMO, and methanotrophy, were shown in this study. The availability of different nutrients is the main factor shaping distinct niches for soil prokaryotes (Finn et al., 2021). Despite the typical influence of physicochemical factors like salinity, pH, temperature, and available substrates on soil methanogenic groups (Webster et al., 2015), our study highlighted that plants have important impacts on methanogenesis. Concerning CH_4 oxidation, n-DAMO and methanotrophic organisms were notably affected by the soil's chemical composition. The relationships between C parameters and denitrifiers can be explained by the majority of known denitrifiers are heterotrophic bacteria that couple organic C oxidation to the stepwise anaerobic reduction of NO_3^- to N_2O or N_2 gases (Damashek and Francis, 2018). In our study, a low TC/NO_3^- ratio increased NO_2^-, N_2O and N_2 production through denitrification as a high C/NO_3^- balance promotes DNRA, as also supported by Stremińska et al. (2012). Additionally, our findings suggest that ANAMMOX might be suppressed in more C-eutrophic environments (Thamdrup and Dalsgaard, 2002). However, in Chinese sites, excessive N was reduced through ANAMMOX, releasing N_2. Variations in the main nutrients in coastal ecosystems drive shifts in process balances.

According to our findings, DNRA and ANAMMOX negatively correlated with denitrification, which, in turn, showed a positive association with N fixation and n-DAMO. This suggests denitrification becomes thermodynamically favourable in the presence of abundant organic matter, thereby outcompeting ANAMMOX (Thamdrup and Dalsgaard, 2002). In anoxic environments with limited electron acceptors and excess electron donors (e.g., organic C), DNRA is energetically preferred over denitrification. Conversely, denitrification becomes more favourable when electron donors are scarce but $NO3^-$ is abundant (Tiedje et al., 1983). Additionally, N_2 fixation is favoured over denitrification in conditions of limited organic matter, either in quantity or quality (Andersson et al., 2014).

Nitrification was higher in the Chinese sites, while denitrification prevailed in the Estonian sites. Minimal NO_3^- in Estonian sites suggested rapid utilisation by denitrifying microorganisms. Studies indicated increased nitrification and denitrification rates in soils hosting active macrofauna or plant communities, enabling oxygen and NO_3^- ventilation in upper soil layers, thus, stimulating respective processes (Damashek and Francis, 2018). In addition, the bare (E0, P0) sites generally showed less potential for various processes due to the absence of plants and their root exudates. The results of the study showed that the genes mediating the same processes, i.e., denitrification second step by *nirK* and *nirS* genes, denitrification last step by *nosZI* and *nosZII* genes, nitrification by bacterial, archaeal and COMAMMOX *amoA*, showed different

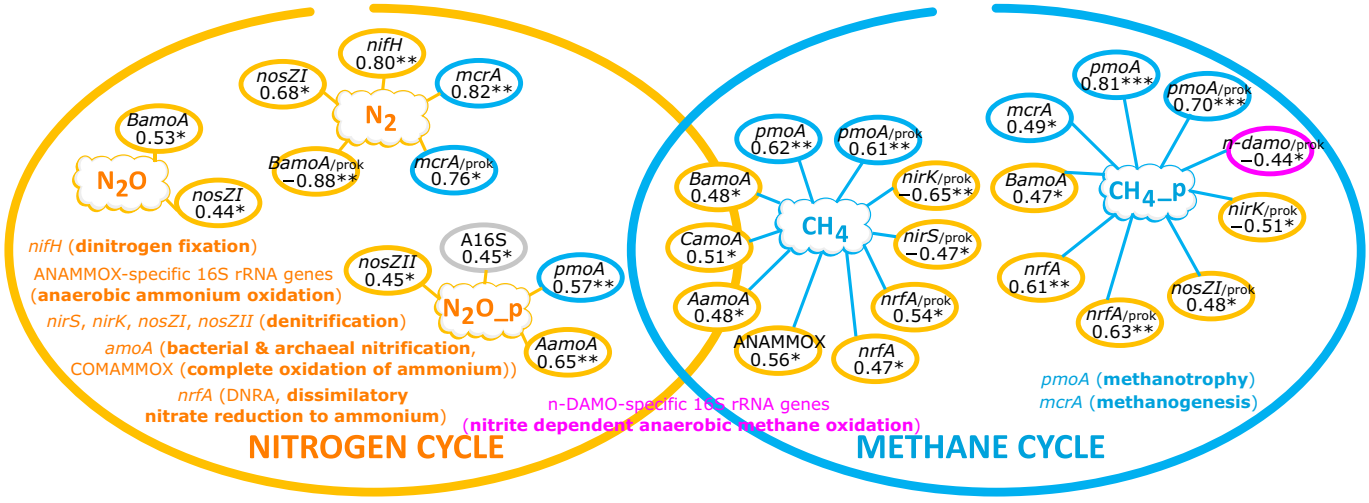

Fig. 4. Integrated view of microbial methane and nitrogen cycles in the coastal ecosystems. Blue color stands for methane cycle processes, orange for nitrogen cycle processes and pink for processes of both cycles. Spearman correlation coefficients (* - $p < 0.05$; ** - $p < 0.01$; *** - $p < 0.001$) between the numbers and proportions of gene copies and gas fluxes in the studied sites. Abbreviations: A16S – archaeal 16S rRNA gene, BamoA – bacterial *amoA*, AamoA – archaeal *amoA*, CamoA – COMAMMOX *amoA*, CH_4 or N_2O – same day emission, CH_4_p or N_2O_p – average emission through the study period.

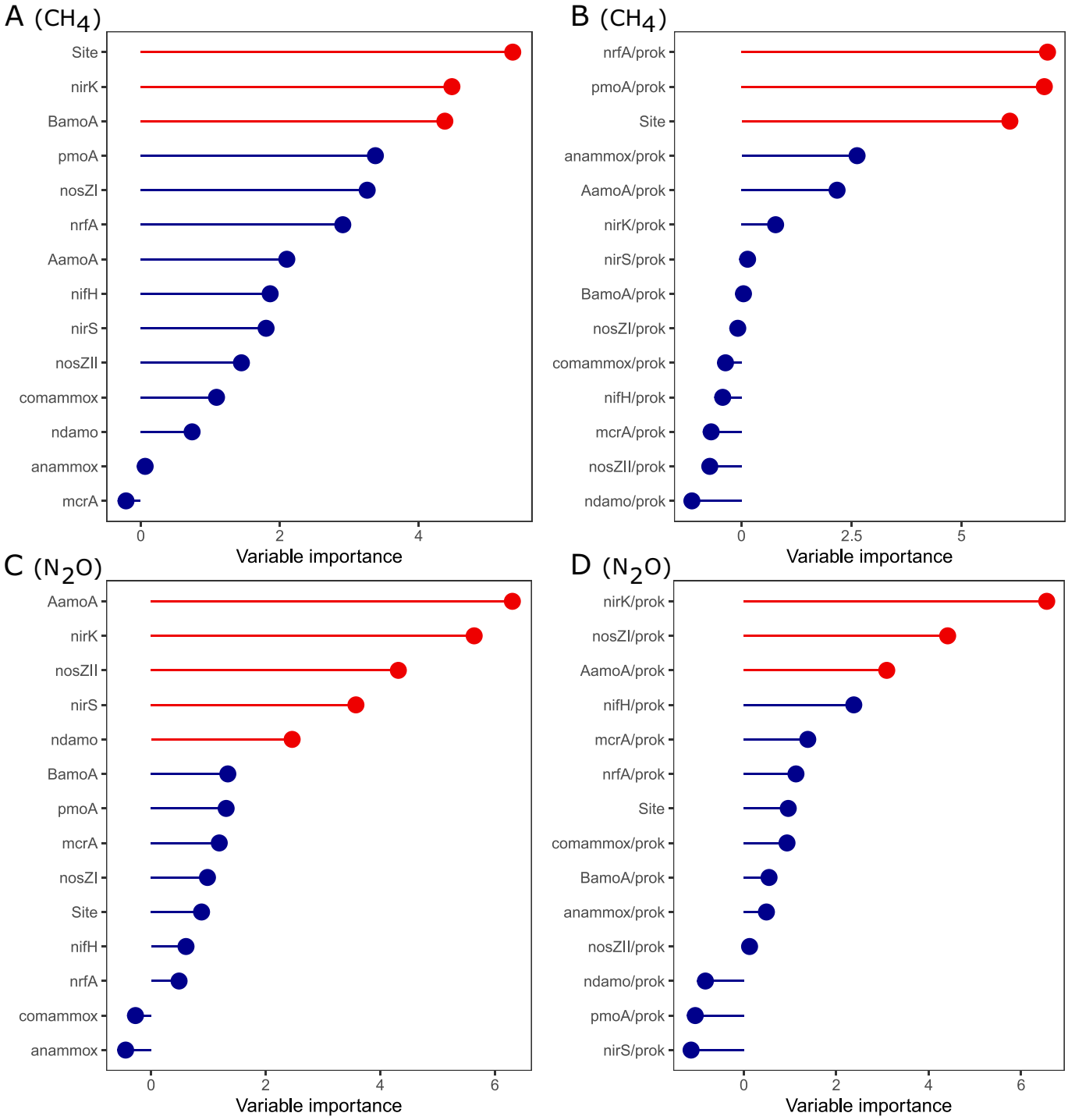

Fig. 5. Random forest analysis results describing the importance of the target gene abundances (A, C) and the target gene proportions in the prokaryotic community (B, D) for methane (A, B) and nitrous oxide (C, D) fluxes. The resulting median of importance was used to order parameters from highest to lowest. The variables in red have statistically significant contributions.

tendencies in responses to environmental parameters, and it was especially clear in the case of *amoA* genes. COMAMMOX process was prevalent in Chinese sites.

The water salinity was an important factor, as it negatively affected denitrification, bacterial nitrification, N fixation and n-DAMO processes but had no impact on archaeal nitrification, COMAMMOX, DNRA and ANAMMOX in N cycle processes. Fortin et al. (2021) noted similar trends in the case of denitrification, and salinity even enhanced DNRA. Moreover, high salinity stress affects both microbes and macrophytes. This stress prompts macrophytes to develop richer roots to extract limited nutrients due to increased N demand (Hsieh et al., 2021), subsequently influencing soil microbiological communities.

4.2. Impacts of coastal plants species on microbial methane and nitrogen cycles in soils

Plants host diverse microbial communities, impacting the success of invasive or native species through complex interactions influenced by

various factors (Dawson and Schrama, 2016). Symbiotic relationships with beneficial microbes enhance host nutrition, growth, and stress resistance, while pathogens exert opposing effects (Kowalski et al., 2015). Plant-associated microbiomes play crucial roles in regulating plant nutrition (Trivedi et al., 2020).

The highest methanogenesis occurred in the old *Spartina*-covered site, where CH_4 emissions were three times higher than in other sites. Limited oxygen transfer from older plants to the rhizosphere inhibits CH_4 oxidation (Jørgensen et al., 2012; Xu et al., 2018). Studies demonstrate that younger, actively growing plants can mitigate greenhouse gas emissions (Cheng et al., 2007; Yang et al., 2020). Despite the higher CH_4 emissions in the older *Spartina* site (P2), no notable differences in methanogen abundance existed between the younger (P3) and older *Spartina* sites (P2). This suggests that the potential for CH_4 production exists, and it is possible that the activity of soil microbes, such as methanogens, may vary during the life cycle of the plants. Additionally, a negative relationship between *mcrA* genes and plant biomass (both above- and belowground) indicates topsoil oxidation by plants and competition between plants and methanogens.

Our results showed n-DAMO process reduced CH_4 emissions. The *Phragmites* (E1) site exhibited the highest abundance of n-DAMO-performing organisms, while the largest proportion within the community was observed in the bare (P0) site on the Chinese coast. The n-DAMO process has also been identified in various natural environments, including freshwater lakes, rivers, and wetlands (Hu et al., 2014; Li-Dong et al., 2014; Shen et al., 2015). However, this process has received limited study to date.

Based on our findings, plants' belowground and aboveground biomass growth reduced N fixers abundance. Plants release up to 20 % of fixed C and 15 % of N into the soil; however, the amount and composition of root exudates vary from simple molecules to complex polymers (e.g., sugars, organic acids, secondary metabolites, and mucilage) (Sasse et al., 2018). Moreover, since the studied plants are not strictly in symbiosis with N-fixing microbes and enough N was available, the plants decreased the performance of the N-fixers.

Bacterial nitrification prevailed in the *Spartina* (P1, P2, P3) sites, while archaeal nitrification was observed in all studied soils under any plants. Some plants might inhibit bacterial and archaeal nitrification by releasing inhibitory compounds in root exudates (Nardi et al., 2020). The COMAMMOX process was preferred in the *Spartina* and *Scirpus* (P1) site but absent in the *Phragmites* (E1) site. COMAMMOX bacteria prefer low NH_4^+ concentrations, avoiding direct competition with bacterial nitrifiers in high NH_4^+ environments. The ecological aspects of COMAMMOX in soil, particularly in coastal sediments (Yu et al., 2018), remain largely unexplored (Daims et al., 2015; Nardi et al., 2020). Anaerobic NH_4^+ oxidation can remove excess N as N_2, thereby reducing potential N_2O emissions. The Chinese (P0, P1, P2, P3) sites displayed the highest genetic potential for ANAMMOX. Conversely, the low genetic potential of ANAMMOX in the *Schoenoplectus* (E2) and *Phragmites* (E1) sites suggests that the bacteria in those locations may necessitate more stable anaerobic conditions and NH_4^+ concentrations (Kuenen, 2008).

Our data reveal extensive denitrification across vegetated sites (*Spartina* (P1, P2, P3), *Phragmites* (E1)), as well as in the Estonian bare (E0) site. These sites also differed statistically significantly in C concentrations, with higher amounts greatly promoting denitrification (Damashek and Francis, 2018). *Spartina* (P2, P3) and *Phragmites* (E1) sites showed higher N_2O emissions compared to the other plant species sites, consistent with prior studies (Cheng et al., 2007; Zhang et al., 2013; Hsieh et al., 2021). These studies indicate that plants enhance the activity of nitrifying and denitrifying microorganisms by enriching the soil with necessary substrates (C and N compounds) during higher biomass periods (Hsieh et al., 2021). However, the opposite relationship could be seen during the dormant period of plants, with competition between soil microbes and plants for reduced nutrients in the soil (Cheng et al., 2007; Yu et al., 2012; Zhang et al., 2013), consistent with observations in our study.

The DNRA process was highest in *Spartina* (P1, P2, P3) sites. This trend aligns with findings in brackish estuarine soils, where increased salinity and temperature reduced denitrification but enhanced microorganisms with the *nrfA* gene activity in sediments (Giblin et al., 2010). Similar observations were noted in various tropical estuaries (Dong et al., 2009). *Phragmites* (E1) sites displayed lower genetic potential for DNRA, suggesting that N was mainly reduced from the soil to the atmosphere due to denitrification.

4.3. Role of greenhouse gases and climate change in coastal ecosystems with different dominating plants

In this study, *Spartina* (P1, P2, P3) sites were the primary emitters of CH_4. Previous studies have indicated higher CH_4 emissions in invasive *Spartina* sites compared to other plants (Hsieh et al., 2021; Derby et al., 2022). The emissions from bare (E0), *Phragmites* (E1), and *Schoenoplectus* (E2) sites were negligible, and the bare (P0) site even showed consumption of CH_4. In various wetlands, it has been observed that in N-rich coastal sediments, methanotrophs consumed atmospheric CH_4 when its concentration in the soil was low (He et al., 2019). As observed in prior research (Cheng et al., 2007; Bridgham et al., 2013; Abdalla et al., 2016), plant species significantly influence CH_4 transport and production. Biomass debris contributes to C sequestration in soils but also promotes CH_4 emissions by stimulating methanogenic archaea (Hsieh et al., 2021). In addition, some CH_4 may escape into the atmosphere through the plants' aerenchyma (Hirota et al., 2004; Koelbener et al., 2010). Wetland plants' roots excrete nutrients that support methanogens in CH_4 formation while transmitting O_2 for growth and CH_4 oxidation (Hsieh et al., 2021). Among all types of wetlands, coastal wetlands typically exhibit lower CH_4 emissions due to seawater tides introducing sulphate, suppressing CH_4 production, and favouring C storage (Andrews et al., 2006). Positive relationships were noted between *mcrA* genes and CH_4 emissions, whereas a negative correlation was found between n-DAMO genes and CH_4 emissions. Freshwater sediment studies have observed CH_4 oxidation coupled with nitrate/nitrite reduction (n-DAMO) by prokaryotes, potentially also aiding in removing CH_4 from coastal marine sediments (Wallenius et al., 2021).

In this study, the biggest emitters of N_2O were sites of *Phragmites* (E1) and old *Spartina* (P2); however, approximately half less N_2O emissions came from sites of a mix of *Spartina* and *Scirpus* (P1) and young *Spartina* (P3). The produced N_2O may also be emitted into the atmosphere via the highly developed aerenchyma of *Spartina* and *Phragmites* (Cheng et al., 2007). Lower N_2O emissions were observed from bare (E0 and P0) and *Schoenoplectus* (E2) sites. Plant species, as seen in CH_4 emission, also influence N_2O transport and production. Additionally, plant age and biomass were factors affecting CH_4 and N_2O emissions; younger plants tended to reduce these emissions into the atmosphere.

The temporal pattern of positive and negative N_2O fluxes associated with plants might be linked to the complex dynamics of tidal variations and N uptake by plants. *Spartina*, known for its strong N absorption capabilities, contributes to N removal within the *Spartina* zone but is influenced by tides (Li et al., 2023). Our *Spartina* site, hosting *Spartina* of moderate age (ca 10 years), possesses substantial biomass not just above the ground but also underground. Additionally, due to high soil moisture in wetlands, the release of N_2 may occasionally exceed the rate of N_2O production, resulting in a net consumption of N_2O and negative fluxes. Also, older *Spartina* may contribute OM to the soil, influencing N availability and microbial processes that lead to the reduction of N_2O. Furthermore, temporal patterns of CH_4 or N_2O fluxes in bare sites may result from various physicochemical factors. The bare wetland soils often have waterlogged conditions, creating anaerobic environments that are conducive to CH_4 production (methanogenesis) but suppressive to N_2O production (i.e., denitrification), and thereby, produce high CH_4 and low N_2O emissions. Also, the absence of vegetation in the bare wetland soils may reduce inputs of OM from plant residues, affecting the availability of C substrates for microbial processes and potentially

favouring CH_4 production over N_2O production.

Nitrification and denitrification are the primary processes driving N_2O emissions in our coastal sites. Plant uptake of N also affects N_2O production mechanisms. High net primary production by plants leads to nutrient release from root systems into the soil, stimulating nitrification and denitrification processes (Hsieh et al., 2021). In addition, high productivity and subsequent remineralisation can inject a substantial amount of "new" NH_4^+ into surface sediments, potentially stimulating nitrification if oxygen is present (Damashek and Francis, 2018). Factors like N compound concentration, O_2 levels, macrophyte density, salinity, and groundwater strongly influence both sediment-to-air and water-to-air N_2O fluxes consistently (Murray et al., 2015).

Relationships between various gene parameters and CH_4 and N_2O emissions showed that different microbes performing different processes also affected each other directly or indirectly. Further investigation is essential to understand the factors driving CH_4- and N_2O-cycling pathways and identify the responsible microorganisms. Integrating knowledge about microbial pathways and geochemical processes will likely enhance the accuracy of predicting CH_4 and N_2O emissions from coastal areas in the future (Damashek and Francis, 2018; Wallenius et al., 2021). Using GWP_{100} values to assess the total climate forcing impact of all GHGs, >93 % of total climate forcing came from CH_4, except for the Chinese bare (P0) site where it was negative, and for *Phragmites* (E1) where almost 60 % of climate forcing came from N_2O. Due to high CH_4 and N_2O emissions, both studied coastal marshes are net climate warmers.

The impact of plant communities on mitigating CH_4 and N_2O emissions and their impact on climate change should not be underestimated. Restoration and management actions in coastal wetlands could effectively mitigate climate change without negatively impacting these ecosystems, and coastal wetland restoration is estimated to deliver 0.3–3.1 Gt CO_2eq y^{-1} in total (Smith et al., 2019). Pruning plants during the growing season may inhibit CH_4 cycle processes but promote N_2O production (Cheng et al., 2007; Kasak et al., 2020), making it essential to recognise the role of plants in the circulation and maintenance of coastal communities.

5. Conclusion

Microorganisms and plants significantly shape the soil environment and control C and N cycles, including CH_4 and N_2O emissions. CH_4 emissions were highest in the order: old *Spartina* (P2) > a mix of *Spartina* and *Scirpus* (P1) > young *Spartina* (P3) > bare (Estonia, E0) > *Schoenoplectus* (E2) > *Phragmites* (E1) > bare (China, P0). N_2O emissions were highest in the order: *Phragmites* (E1) > old *Spartina* (P2) > a mix of *Spartina* and *Scirpus* (P1) > young *Spartina* (P3) > *Schoenoplectus* (E2) > bare (China, P0) > bare (Estonia, E0). Chinese sites favoured N_2O emissions due to nitrification, while in Estonia, incomplete denitrification led to N_2O emissions. This study reveals complex interactions among microbial processes, indicating their coexistence and competition that influence gas fluxes. The presence of plants impacted the abundance of N fixers, and younger plants reduced CH_4 and N_2O emissions. The study emphasises the importance of studying the soil-plant-atmosphere continuum to understand GHG emissions, with CH_4 being the dominant contributor to total climate forcing, except for the Chinese bare site and *Phragmites australis*, where N_2O played a significant role.

Funding

The research was supported by the Ministry of Education and Research of Estonia (grants IUT2-16, PRG-352, PRG-2032 and MOBERC-20), the EU through the European Regional Development Fund (Centres of Excellence EcolChange), SuperG (funded under EU Horizon 2020 programme), the EU Horizon programme under grant agreement No 101079192 (MLTOM23003R) and the European Research Council (ERC) under grant agreement No 101096403 (MLTOM23415R); the National Key Research and Development Program of China (2016YFE0133700), the National Natural Science Foundation of China (42141016), the Fundamental Research Funds for the Central Universities, the State Key Lab of Estuarine and Coastal Research (SKLEC-DWJS201802), the 111 Project (BP0820020), Ministry of Education, China, East China Normal University ("Ecology+" project and Scholarship Program for Graduate Students—Short-term overseas research scholarship).

CRediT authorship contribution statement

Mikk Espenberg: Writing – review & editing, Writing – original draft, Visualization, Methodology, Investigation, Formal analysis, Data curation, Conceptualization. **Kristin Pille:** Investigation, Formal analysis, Data curation. **Bin Yang:** Methodology, Investigation, Data curation. **Martin Maddison:** Writing – review & editing, Methodology, Investigation, Data curation. **Mohamed Abdalla:** Writing – review & editing. **Pete Smith:** Writing – review & editing. **Xiuzhen Li:** Writing – review & editing, Conceptualization. **Ping-Lung Chan:** Writing – review & editing. **Ülo Mander:** Writing – review & editing, Conceptualization.

Declaration of competing interest

The authors declare that they have no known competing financial interests or personal relationships that could have appeared to influence the work reported in this paper.

Data availability

Data will be made available on request.

Appendix A. Supplementary data

Supplementary data to this article can be found online at https://doi.org/10.1016/j.scitotenv.2024.170641.

References

Abdalla, M., Hasting, A., Truu, J., Espenberg, M., Mander, Ü., Smith, P., 2016. Emissions of methane from northern peatlands: a review of management impacts and implications for future management options. Ecol. Evol. 6, 7080–7102. https://doi.org/10.1002/ece3.2469.

Al-Haj, A.N., Fulweiler, R.W., 2020. A synthesis of methane emissions from shallow vegetated coastal ecosystems. Glob. Chang. Biol. 26 (5), 2988–3005. https://doi.org/10.1111/gcb.15046.

Andersson, B., Sundbäck, K., Hellman, M., Hallin, S., Alsterberg, C., 2014. Nitrogen fixation in shallow-water sediments: spatial distribution and controlling factors. Limnol. Oceanogr. 59 (6), 1932–1944. https://doi.org/10.4319/lo.2014.59.6.1932.

Andrews, J.E., Burgess, D., Cave, R.R., Coombes, E.G., Jickells, T.D., Parkes, D.J., et al., 2006. Biogeochemical value of managed realignment, Humber estuary, UK. Sci. Total Environ. 371, 19–30. https://doi.org/10.1016/j.scitotenv.2006.08.021.

APHA-AWWA-WEF, 2005. Standard Methods for the Examination of Water and Wastewater, 21th ed. American Public Health Organisation.

Bahram, M., Espenberg, M., Pärn, J., Lehtovirta-Morley, L., Anslan, S., Kasak, K., et al., 2022. Structure and function of the soil microbiome underlying N_2O emissions from global wetlands. Nat. Commun. 13 (1), 1430. https://doi.org/10.1038/s41467-022-29161-3.

Bates, D., Mächler, M., Bolker, B., Walker, S., 2015. Fitting linear mixed-effects models using lme4. J. Stat. Softw. 67 https://doi.org/10.18637/jss.v067.i01.

Bauer, J.E., Cai, W.J., Raymond, P.A., Bianchi, T.S., Hopkinson, C.S., Regnier, P.A., 2013. The changing carbon cycle of the coastal ocean. Nature 504 (7478), 61–70. https://doi.org/10.1038/nature12857.

Bernhardt, J.R., Leslie, H.M., 2013. Resilience to climate change in coastal marine ecosystems. Annu. Rev. Mar. Sci. 5, 371–392. https://doi.org/10.1146/annurev-marine-121211-172411.

Bridgham, S.D., Cadillo-Quiroz, H., Keller, J.K., Zhuang, Q., 2013. Methane emissions from wetlands: biogeochemical, microbial, and modeling perspectives from local to global scales. Glob. Chang. Biol. 19 (5), 1325–1346. https://doi.org/10.1111/gcb.12131.

Bruns, A., 2014. The environmental impacts of megacities on the coast. In: Pelling, M., Blackburn, S. (Eds.), Megacities and the Coast. Routledge, Abingdon, Oxon, NY, pp. 46–93. https://doi.org/10.4324/9780203066423.

Burden, A., Smeaton, C., Angus, S., Garbutt, A., Jones, L., Lewis, H., et al., 2020. Impacts of climate change on coastal habitats, relevant to the coastal and marine environment around the UK. MCCIP Sci. Rev. 2020, 228–255. https://doi.org/10.14465/2020.arc11.chb.

Butterbach-Bahl, K., Willibald, G., Papen, H., 2002. Soil core method for direct simultaneous determination of N_2 and N_2O-emissions from forest soil. Plant Soil 240, 105–116. https://doi.org/10.1023/A:1015870518723.

Cavicchioli, R., Ripple, W.J., Timmis, K.N., Azam, F., Bakken, L.R., Baylis, M., et al., 2019. Scientists' warning to humanity: microorganisms and climate change. Nat. Rev. Microbiol. 17 (9), 569–586. https://doi.org/10.1038/s41579-019-0222-5.

Cheng, X., Peng, R., Chen, J., Luo, Y., Zhang, Q., An, S., et al., 2007. CH_4 and N_2O emissions from *Spartina alterniflora* and *Phragmites australis* in experimental mesocosms. Chemosphere 68, 420–427. https://doi.org/10.1016/j.chemosphere.2007.01.004.

Craig-Smith, S.J., Tapper, R., Font, X., 2006. In: Gössling, S., Hall, C.M. (Eds.), "The Coastal and Marine Environment" in Tourism and Global Environmental Change: Ecological, Social, Economic and Political Interrelationships. Routledge, Abingdon, Oxon, NY, pp. 107–127. https://doi.org/10.4324/9780203011911.

Daims, H., Lebedeva, E.V., Pjevac, P., Han, P., Herbold, C., Albertsen, M., et al., 2015. Complete nitrification by *Nitrospira* bacteria. Nature 528, 504–509. https://doi.org/10.1038/nature16461.

Damashek, J., Francis, C.A., 2018. Microbial nitrogen cycling in estuaries: from genes to ecosystem processes. Estuaries Coast 41 (3), 626–660. https://doi.org/10.1007/s12237-017-0306-2.

Dawson, W., Schrama, M., 2016. Identifying the role of soil microbes in plant invasions. J. Ecol. 104 (5), 1211–1218. https://doi.org/10.1111/1365-2745.12619.

Deegan, L.A., Johnson, D.S., Warren, R.S., Peterson, B.J., Fleeger, J.W., Fagherazzi, S., et al., 2012. Coastal eutrophication as a driver of salt marsh loss. Nature 490 (7420), 388–392. https://doi.org/10.1038/nature11533.

Derby, R.K., Needelman, B.A., Roden, A.A., Megonigal, J.P., 2022. Vegetation and hydrology stratification as proxies to estimate methane emission from tidal marshes. Biogeochemistry 157 (2), 227–243. https://doi.org/10.1007/s10533-021-00870-z.

Dong, L.F., Smith, C.J., Papaspyrou, S., Stott, A., Osborn, A.M., Nedwell, D.B., 2009. Changes in benthic denitrification, nitrate ammonification, and anammox process rates and nitrate and nitrite reductase gene abundances along an estuarine nutrient gradient (the Colne estuary, United Kingdom). Appl. Environ. Microbiol. 75, 3171–3179. https://doi.org/10.1128/AEM.02511-08.

Dray, S., Dufour, A.B., 2007. The ade4 package: implementing the duality diagram for ecologists. J. Stat. Softw. 22, 1–20. https://doi.org/10.18637/jss.v022.i04.

Finn, D.R., Bergk-Pinto, B., Hazard, C., Nicol, G.W., Tebbe, C.C., Vogel, T.M., 2021. Functional trait relationships demonstrate life strategies in terrestrial prokaryotes. FEMS Microbiol. Ecol. 97 (5), fiab068 https://doi.org/10.1093/femsec/fiab068.

Fortin, S.G., Song, B., Anderson, I.C., 2021. Microbially mediated nitrogen removal and retention in the York River Estuary. FEMS Microbiol. Ecol. 97 (9), fiab118 https://doi.org/10.1093/femsec/fiab118.

Giblin, A.E., Weston, N.B., Banta, G.T., Tucker, J., Hopkinson, C.S., 2010. The effects of salinity on nitrogen losses from an oligohaline estuarine sediment. Estuar. Coasts 33, 1054–1068. https://doi.org/10.1007/s12237-010-9280-7.

Gribben, P.E., Nielsen, S., Seymour, J.R., Bradley, D.J., West, M.N., Thomas, T., 2017. Microbial communities in marine sediments modify success of an invasive macrophyte. Sci. Rep. 7 (1), 1–8. https://doi.org/10.1038/s41598-017-10231-2.

Guibert, L.M., Loviso, C.L., Borglin, S., Jansson, J.K., Dionisi, H.M., Lozada, M., 2016. Diverse bacterial groups contribute to the alkane degradation potential of chronically polluted subantarctic coastal sediments. Microb. Ecol. 71 (1), 100–112. https://doi.org/10.1007/s00248-015-0698-0.

He, Z., Wang, J., Hu, J., Yu, H., Jetten, M.S., Liu, H., et al., 2019. Regulation of coastal methane sinks by a structured gradient of microbial methane oxidizers. Environ. Pollut. 244, 228–237. https://doi.org/10.1016/j.envpol.2018.10.057.

Herbert, R.A., 1999. Nitrogen cycling in coastal marine ecosystems. FEMS Microbio. Rev. 23 (5), 563–590. https://doi.org/10.1111/j.1574-6976.1999.tb00414.x.

Hirota, M., Tang, Y., Hu, Q., Hirata, S., Kato, T., Mo, W., et al., 2004. Methane emissions from different vegetation zones in a Qinghai-Tibetan plateau wetland. Soil Biol. Biochem. 36 (5), 737–748. https://doi.org/10.1016/j.soilbio.2003.12.009.

Hsieh, S.H., Yuan, C.S., Ie, I.R., Yang, L., Lin, H.J., Hsueh, M.L., 2021. In-situ measurement of greenhouse gas emissions from a coastal estuarine wetland using a novel continuous monitoring technology: comparison of indigenous and exotic plant species. J. Environ. Manag. 281, 111905 https://doi.org/10.1016/j.jenvman.2020.111905.

Hu, B.L., Shen, L.D., Lian, X., Zhu, Q., Liu, S., Huang, Q., et al., 2014. Evidence for nitrite-dependent anaerobic methane oxidation as a previously overlooked microbial methane sink in wetlands. Proc. Natl. Acad. Sci. 111, 4495–4500. https://doi.org/10.1073/pnas.1318393111.

in't Zandt, M.H., de Jong, A.E., Slomp, C.P., Jetten, M.S., 2018. The hunt for the most-wanted chemolithoautotrophic spookmicrobes. FEMS Microbiol. Ecol. 94 (6), fiy064 https://doi.org/10.1093/femsec/fiy064.

IPCC, 2021. In: Masson-Delmotte, V., Zhai, P., Pirani, A., Connors, S.L., Péan, C., Berger, S., et al. (Eds.), Climate Change 2021: The Physical Science Basis. Contribution of Working Group I to the Sixth Assessment Report of the Intergovernmental Panel on Climate Change. Cambridge University Press. https://doi.org/10.1017/9781009157896.001.

Jansson, J.K., Hofmockel, K.S., 2020. Soil microbiomes and climate change. Nat. Rev. Microbiol. 18 (1), 35–46. https://doi.org/10.1038/s41579-019-0265-7.

Jaspers, C., Bezio, N., Hinrichsen, H.H., 2021. Diversity and physiological tolerance of native and invasive jellyfish/ctenophores along the extreme salinity gradient of the Baltic Sea. Diversity 13 (2), 57. https://doi.org/10.3390/d13020057.

Jørgensen, C.J., Struwe, S., Elberling, B., 2012. Temporal trends in N_2O flux dynamics in a Danish wetland - effects of plant-mediated gas transport of N_2O and O_2 following changes in water level and soil mineral-N availability. Glob. Chang. Biol. 18, 210–222. https://doi.org/10.1111/j.1365-2486.2011.02485.x.

Kasak, K., Valach, A.C., Rey-Sanchez, C., Kill, K., Shortt, R., Liu, J., et al., 2020. Experimental harvesting of wetland plants to evaluate trade-offs between reducing methane emissions and removing nutrients accumulated to the biomass in constructed wetlands. Sci. Total Environ. 715, 136960 https://doi.org/10.1016/j.scitotenv.2020.136960.

Koelbener, A., Ström, L., Edwards, P.J., Venterink, H.O., 2010. Plant species from mesotrophic wetlands cause relatively high methane emissions from peat soil. Plant Soil 326 (1–2), 147–158. https://doi.org/10.1007/s11104-009-9989-x.

Kowalski, K.P., Bacon, C., Bickford, W., Braun, H., Clay, K., Leduc-Lapierre, M., et al., 2015. Advancing the science of microbial symbiosis to support invasive species management: a case study on Phragmites in the Great Lakes. Front. Microbiol. 6, 95. https://doi.org/10.3389/fmicb.2015.00095.

Kuenen, J.G., 2008. Anammox bacteria: from discovery to application. Nat. Rev. Microbiol. 6 (4), 320–326. https://doi.org/10.1038/nrmicro1857.

Kursa, M.B., Rudnicki, W.R., 2010. Feature selection with the Boruta package. J. Stat. Softw. 36, 1–13.

Kuznetsova, A., Brockhoff, P.B., Christensen, R.H.B., 2017. lmerTest package: tests in linear mixed effects models. J. Stat. Softw. 82 https://doi.org/10.18637/jss.v036.i11.

Lapointe, B.E., Herren, L.W., Debortoli, D.D., Vogel, M.A., 2015. Evidence of sewage-driven eutrophication and harmful algal blooms in Florida's Indian River lagoon. Harmful Algae 43, 82–102. https://doi.org/10.1016/j.hal.2015.01.004.

Li, Z., Li, X., Tan, L., Yan, Z., 2023. Nutrient reduction effect of different vegetation types at the Nanhui tidal flat of Yangtze Estuary. Chin. J. Ecol. 42 (2), 375.

Li-Dong, S., Qun, Z., Shuai, L., Ping, D., Jiang-Ning, Z., Dong-Qing, C., et al., 2014. Molecular evidence for nitrite-dependent anaerobic methane-oxidizing bacteria in the Jiaojiang estuary of the East Sea (China). Appl. Microbiol. Biotechnol. 98, 5029–5038. https://doi.org/10.1007/s00253-014-5556-3.

Liu, Z., Fagherazzi, S., Cui, B., 2021. Success of coastal wetlands restoration is driven by sediment availability. Commun. Earth Environ. 2 (1), 1–9. https://doi.org/10.1038/s43247-021-00117-7.

Loftfield, N., Flessa, H., Augustin, J., Beese, F., 1997. Automated gas chromatographic system for rapid analysis of the atmospheric trace gases methane, carbon dioxide, and nitrous oxide. J. Environ. Qual. 26 (2), 560–564. https://doi.org/10.2134/jeq1997.00472425002600020030x.

Murray, R.H., Erler, D.V., Eyre, B.D., 2015. Nitrous oxide fluxes in estuarine environments: response to global change. Glob. Chang. Biol. 21 (9), 3219–3245. https://doi.org/10.1111/gcb.12923.

Nardi, P., Laanbroek, H.J., Nicol, G.W., Renella, G., Cardinale, M., Pietramellara, G., et al., 2020. Biological nitrification inhibition in the rhizosphere: determining interactions and impact on microbially mediated processes and potential applications. FEMS Microbiol. Rev. 44 (6), 874–908. https://doi.org/10.1093/femsre/fuaa037.

Newton, A., Icely, J., Cristina, S., Perillo, G.M., Turner, R.E., Ashan, D., et al., 2020. Anthropogenic, direct pressures on coastal wetlands. Front. Ecol. Evol. 8, 144. https://doi.org/10.3389/fevo.2020.00144.

Novoa, A., Keet, J.H., Lechuga-Lago, Y., Pyšek, P., Roux, J.J.L., 2020. Urbanization and *Carpobrotus edulis* invasion alter the diversity and composition of soil bacterial communities in coastal areas. FEMS Microbiol. Ecol. 96 (7), fiaa106 https://doi.org/10.1093/femsec/fiaa106.

Oksanen J, Blanchet FG, Friendly M, Kindt R, Legendre P, McGlinn D, et al. 2020. Vegan: Community Ecology Package.

Paerl, H.W., Dennis, R.L., Whitall, D.R., 2002. Atmospheric deposition of nitrogen: implications for nutrient over-enrichment of coastal waters. Estuaries 25 (4), 677–693. https://doi.org/10.1007/BF02804899.

Quick, A.M., Reeder, W.J., Farrell, T.B., Tonina, D., Feris, K.P., Benner, S.G., 2019. Nitrous oxide from streams and rivers: A review of primary biogeochemical pathways and environmental variables. Earth Sci. Rev. 191, 224–262. https://doi.org/10.1016/j.earscirev.2019.02.021.

R Core Team, 2021. R: A Language and Environment for Statistical Computing.

Ruijter, J.M., Ramakers, C., Hoogaars, W.M.H., Karlen, Y., Bakker, O., Van den Hoff, M.J.B., et al., 2009. Amplification efficiency: linking baseline and bias in the analysis of quantitative PCR data. Nucleic Acids Res. 37 (6), e45 https://doi.org/10.1093/nar/gkp045.

Sasse, J., Martinoia, E., Northen, T., 2018. Feed your friends: do plant exudates shape the root microbiome? Trends Plant Sci. 23 (1), 25–41. https://doi.org/10.1016/j.tplants.2017.09.003.

Saunois, M., Stavert, A.R., Poulter, B., Bousquet, P., Canadell, J.G., Jackson, R.B., et al., 2020. The global methane budget 2000–2017. Earth Syst. Sci. Data 12, 1561–1623. https://doi.org/10.5194/essd-12-1561-2020.

Shen, L.D., Wu, H.S., Gao, Z.Q., 2015. Distribution and environmental significance of nitrite-dependent anaerobic methane-oxidising bacteria in natural ecosystems. Appl. Microbiol. Biotechnol. 99, 133–142. https://doi.org/10.1007/s00253-014-6200-y.

Smith, P., Calvin, K., Nkem, J., Campbell, D., Cherubini, F., Grassi, G., et al., 2019. Which practices co-deliver food security, climate change mitigation and adaptation, and combat land degradation and desertification? Glob. Chang. Biol. 26, 1532–1575. https://doi.org/10.1111/gcb.14878.

Stremińska, M.A., Felgate, H., Rowley, G., Richardson, D.J., Baggs, E.M., 2012. Nitrous oxide production in soil isolates of nitrate-ammonifying bacteria. Environ. Microbiol. Rep. 4 (1), 66–71. https://doi.org/10.1111/j.1758-2229.2011.00302.x.

Swerts, M., Uytterhoeven, G., Merckx, R., Vlassak, K., 1995. Semicontinuous measurement of soil atmosphere gases with gas-flow soil core method. Soil Sci. Soc.

Am. J. 59, 1336–1342. https://doi.org/10.2136/sssaj1995.03615995005900050020x.
Thamdrup, B., Dalsgaard, T., 2002. Production of N_2 through anaerobic ammonium oxidation coupled to nitrate reduction in marine sediments. Appl. Environ. Microbiol. 68 (3), 1312–1318. https://doi.org/10.1128/AEM.68.3.1312-1318.2002.
Tiedje, J.M., Sexstone, A.J., Myrold, D.D., Robinson, J.A., 1983. Denitrification: ecological niches, competition and survival. Antonie Van Leeuwenhoek 48 (6), 569–583. https://doi.org/10.1007/BF00399542.
Trivedi, P., Leach, J.E., Tringe, S.G., Sa, T., Singh, B.K., 2020. Plant–microbiome interactions: from community assembly to plant health. Nat. Rev. Microbiol. 18 (11), 607–621. https://doi.org/10.1038/s41579-020-0412-1.
Wallenius, A.J., Dalcin Martins, P., Slomp, C.P., Jetten, M.S., 2021. Anthropogenic and environmental constraints on the microbial methane cycle in coastal sediments. Front. Microbiol. 12, 293. https://doi.org/10.3389/fmicb.2021.631621.
Webster, G., O'Sullivan, L.A., Meng, Y., Williams, A.S., Sass, A.M., Watkins, A.J., et al., 2015. Archaeal community diversity and abundance changes along a natural salinity gradient in estuarine sediments. FEMS Microbiol. Ecol. 91, fiu025 https://doi.org/10.1093/femsec/fiu025.
Winter, G., Hetzel, Y., Huang, P., Hipsey, M.R., Mulligan, R.P., Hansen, J., 2019. Coastal processes, extreme events and forecasting. In: Techera, E.J., Winter, G. (Eds.), Marine Extremes: Ocean Safety, Marine Health and the Blue Economy. Routledge, Abingdon, Oxon, NY, pp. 31–47.
Xu, S., Lu, W., Muhammad, F.M., Liu, Y., Guo, H., Meng, R., et al., 2018. New molecular method to detect denitrifying anaerobic methane oxidation bacteria from different environmental niches. J. Environ. Sci. 65, 367–374. https://doi.org/10.1016/j.jes.2017.04.016.
Yang, B., Li, X., Lin, S., Xie, Z., Yuan, Y., Espenberg, M., et al., 2020. Invasive *Spartina alterniflora* can mitigate N_2O emission in coastal salt marshes. Ecol. Eng. 147, 105758 https://doi.org/10.1016/j.ecoleng.2020.105758.
Yang, B., Li, X., Lin, S., Jiang, C., Xue, L., Wang, J., et al., 2021. Invasive *Spartina alterniflora* changes the Yangtze estuary salt marsh from CH_4 sink to source. Estuar. Coast. Shelf Sci. 252, 107258 https://doi.org/10.1016/j.ecss.2021.107258.
Yu, Z., Li, Y., Deng, H., Wang, D., Chen, Z., Xu, S., 2012. Effect of *Scirpus mariqueter* on nitrous oxide emissions from a subtropical monsoon estuarine wetland. Eur. J. Vasc. Endovasc. Surg. 117, G02017 https://doi.org/10.1029/2011JG001850.
Yu, C., Hou, L., Zheng, Y., Liu, M., Yin, G., Gao, J., et al., 2018. Evidence for complete nitrification in enrichment culture of tidal sediments and diversity analysis of clade a comammox *Nitrospira* in natural environments. Appl. Microbiol. Biotechnol. 102 (21), 9363–9377. https://doi.org/10.1007/s00253-018-9274-0.
Zhang, Y., Wang, L., Xie, X., Huang, L., Wu, Y., 2013. Effects of invasion of *Spartina alterniflora* and exogenous N deposition on N_2O emissions in a coastal salt marsh. Ecol. Eng. 58, 77–83. https://doi.org/10.1016/j.ecoleng.2013.06.011.
Zhu, Z., Vuik, V., Visser, P.J., Soens, T., van Wesenbeeck, B., van de Koppel, J., et al., 2020. Historic storms and the hidden value of coastal wetlands for nature-based flood defence. Nat. Sustain. 3 (10), 853–862. https://doi.org/10.1038/s41893-020-0556-z.